Tailoring the switching performance of resistive switching SrTiO₃ devices by SrO interface engineering

F.V.E. Hensling*, T. Heisig, N. Raab, C. Baeumer, R. Dittmann

PGI 7 and JARA-FIT, Forschungszentrum Jülich, Germany

ARTICLE INFO

ABSTRACT

Redox-based resistive switching is one of the most-promising concepts in the focus of research to meet the ever-growing demand for faster and smaller non-volatile memory devices. In this work we present detailed studies of the impact of cation stoichiometry and surface segregation effects on the performance of the valence change memory model material $SrTiO_3$. In order to clarify if the enhanced switching performance of Sr-rich $SrTiO_3$ devices can be attributed to SrO segregation or to the formation of Sr-rich extended defects, we artificially engineered the formation of SrO islands by depositing additional SrO on top of stoichiometric $SrTiO_3$. We thereby unravel that the enhanced switching performance is solely accounted for by the formation of SrO islands and not influenced by extended defects. Consequently following our findings, we design devices with a further improved retention by tailoring the amount of SrO on the surface.

1. Introduction

A central challenge in today's electrical engineering and research community is the need for faster, smaller and energy efficient non-volatile memory devices. A potential candidate for realizing such devices is the mechanism of resistive switching, which even allows multibit operation, logic-in-memory applications, and neuromorphic computing architectures [1–6]. It is based on the reversible change of the resistance of an active material between two electrodes by applying electrical stimuli. $SrTiO_3$ (STO) is an intensely investigated model material for filamentary resistive switching transition metal oxides [7–9]. It is well established that the switching between the high resistive state (HRS) and the low resistive state (LRS) is based on the modulation of the oxygen content within oxygen-vacancy-rich conducting filaments [10–14].

We have previously shown that so-called eightwise resistive switching in STO thin films (switching into the LRS with positive bias applied to the Schottky-type interface) can be explained by reversible release and reincorporation of oxygen in the filament region either stored in or beneath the Pt or supplied by the atmosphere [15,16], in contrast to counter-eightwise switching (switching into the LRS with negative bias applied to the Schottky-type interface), which is usually explained by an internal rearrangement of oxygen vacancies [17]. It has been shown that stoichiometric STO cells usually exhibit a relatively short retention time of the LRS [10,18–20], due to the reoxidation of

the conducting filament over time [10]. In contrast, we have previously shown that using Sr-rich STO shows an enhanced LRS retention [19].

One possible explanation for this phenomenon could be that extended defects such as antiphase boundaries present in Sr-rich thin films [21,22] stabilize oxygen vacancies [19]. This would be consistent with reports in the literature that polycrystalline STO thin films with increased defect density show an improved LRS retention [23].

Another explanation for the enhanced LRS retention of Sr-rich STO is the formation of SrO islands during growth [24,25] or switching, as SrO is a diffusion barrier for oxygen. This explains why the formation of SrO segregations may protect the vacancy-rich filaments from reoxidation by ambient oxygen, thus leading to improved retention times [10].

In this work we clarify if the enhanced performance of Sr-rich STO can be solely explained by the SrO surface segregation during switching or growth. To this end, we systematically introduce different thicknesses of SrO as retention-stabilization layers at the oxide/electrode interface. Thus, we are able to mimic the superior switching behavior of Sr-rich STO compared to stoichiometric STO and derive means to further improve its performance.

2. Materials and methods

20 nm epitaxial STO thin films were grown by pulsed laser deposition (PLD) on TiO_2-terminated [26] 0.5 wt% Nb:STO substrates. This

---

offers the advantage of simultaneously functioning as a conductive bottom electrode. The substrate temperature was 800 °C and the oxygen pressure during deposition was 0.1 mbar to achieve high quality STO thin films. Varying the energy density of the laser, Sr-rich (Sr / (Sr + Ti) ≈ 0.53) and stoichiometric STO was grown, using a fluence of 0.63 J/cm^2 and 1.02 J/cm^2, respectively [24,25,27,28]. SrO was grown ablating a SrO$_2$ target with a laser fluence of 0.81 J/cm^2 at a substrate temperature of 800 °C and an oxygen pressure of 10^{-7} mbar. The target substrate distance was constantly 44 mm. The topography of these thin films was analyzed using a *SIS Pico Station UltraObjective* atomic force microscope (AFM). Subsequently 30 nm Pt were evaporated as top electrode. The Pt was patterned into $10 \times 10 \, \mu m^2$ square top electrodes using photolithography and Ar ion beam etching. The devices fabricated in this manner are electrically characterized using a *Keithley 2611A Source Meter*, bottom electrode grounded, top electrode contacted with W whisker probes. At all times, a current compliance of 10 mA was applied. Read outs were performed at 0.1 V, formation and switching into the LRS (SET) were done at +3 V, the switching into the HRS (RESET) at −4 V.

3. Results

Fig. 1 shows the topography of the as-grown thin films acquired *via* AFM of a) a stoichiometric thin film and b) a Sr-rich thin film. The stoichiometric STO is atomically flat, while the Sr-rich STO film shows SrO islands [24,25].

In order to emulate the SrO segregation of Sr-rich thin films, we deposited additional SrO after the deposition of a 20 nm thick stoichiometric thin film. Fig. 1f) shows the reflective high energy electron diffraction (RHEED) oscillations for the growth of SrO. Due to the higher atom form factor of Sr in comparison to Ti a maximum in the intensity of the secondary spots (blue and green) corresponds to a SrO termination [29–31]. The oscillation of secondary spots and the additional oscillation of the main spot (red) thus correspond to the layer-by-layer growth of 1.5 unit cells (u.c.) [31].

Further deposition of SrO results in the formation of SrO islands, shown for 2 u.c. in Fig. 1d) and 3 u.c. in Fig. 1e). The increase of the thickness of the additional SrO results in a higher SrO island density, while the individual islands show a similar height. The increased surface roughness results in the vanishing of the RHEED signal (Fig. 1f)). The transition to 3D growth can be explained by the different lattice parameters of STO and SrO. While SrO has a rock salt structure with a = 0.51 nm, STO is a perovskite with a = 0.39 nm [32–34]. The high lattice mismatch results in a high stress, which in turn results in a transition to 3D growth to decrease the stress.

The layer-by-layer growth of the initial 1.5 u.c. in turn can be explained by a mere termination conversion from the TiO$_2$-termination towards a SrO-termination. The additional 0.5 u.c. are equivalent to a stacking error at the surface.

Successfully having deposited STO and SrO, we subsequently evaporated Pt on top and patterned it into $10 \times 10 \, \mu m^2$ electrodes. The resulting devices were carefully electrically characterized. The results are depicted in Fig. 2.

Fig. 2a) shows the typical forming (red) and SET (blue) of stoichiometric STO. Fig. 2b) shows the same for Sr-rich STO. As previously reported, Sr-rich STO has a more pronounced forming step, which we will discuss later [19]. Considering the forming and SET of the stoichiometric device with an additional 3 u.c. of SrO (Fig. 2c)) it is conspicuous that the same pronounced forming step can be observed. The similarity of the *I(V)*-characteristics for the Sr-rich STO devices and the devices with intentionally inserted SrO is a first hint towards the same underlying mechanism. For both a significant current only starts at the comparably high voltage of 1 V (compare stoichiometric: 0.5 V).

Fig. 2d) shows the LRS resistance immediately after the SET. The error bars in Fig. 2d) and e) correspond to the standard deviation of at least six switched devices. The stoichiometric devices (black) have the
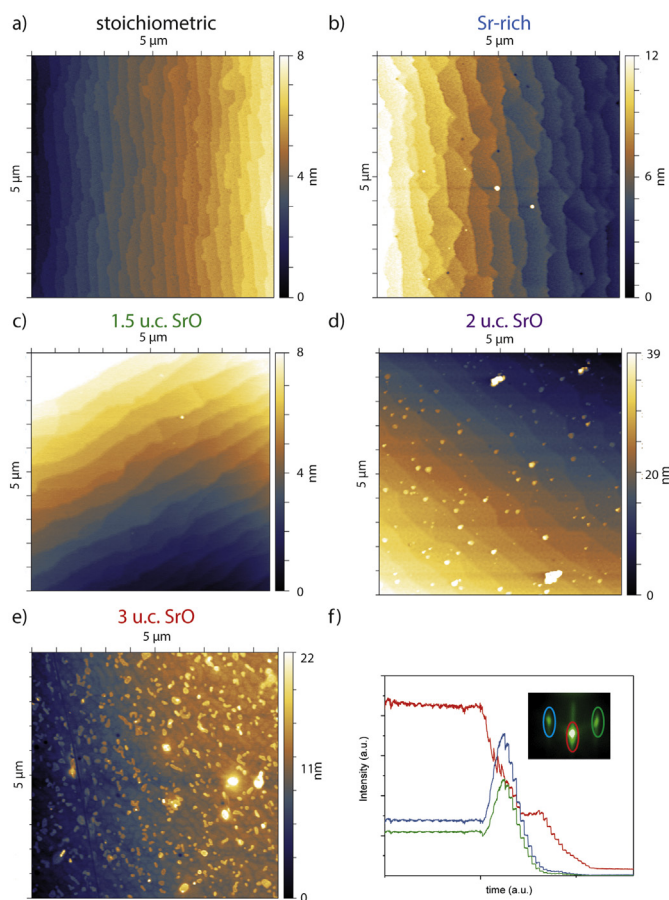

Fig. 1. AFM topography images of a) stoichiometric STO, b) Sr-rich STO c) 1.5 u.c. of SrO deposited on top of a stoichiometric thin film, d) 2 u.c. and e) 3 u.c., respectively. The stoichiometric thin film is atomically flat, as is the thin film with an additional 1.5 u.c. of SrO. Sr-rich STO shows the formation of small confined islands. The deposition of 2 u.c. SrO or more results in the formation of islands of various sizes. f) Shows the RHEED oscillation recorded during the deposition of SrO. The inset shows the RHEED pattern corresponding to the oscillations. (For interpretation of the references to colour in this figure, the reader is referred to the web version of this article.)

highest LRS and the lowest HRS (Fig. 2e) black HRS). The LRS of the Sr-rich devices (blue) is one order of magnitude lower and the HRS (Fig. 2e) blue HRS) is one order of magnitude higher, in agreement with our previous work [19]. Their memory window is thus two orders of magnitude larger. All devices with additional SrO at the Pt/STO interface show an even lower LRS resistance. Taking the error into account, the LRS of devices with additional SrO at the Pt/STO interface appears to be rather independent of the thickness of the SrO. Their HRS, however is lower than that of the Sr-rich devices (Fig. 2e) black HRS). They have thus a similar memory window as Sr-rich devices.

Although the LRS resistance measured immediately after the SET is independent of the SrO thickness, the LRS retention in Fig. 2e) is directly affected by it. While samples with an additional 1.5 u.c. of SrO (green) show a similar retention as stoichiometric devices (black), samples with an additional 2 u.c. SrO (pink) show a similar retention behavior as Sr-rich devices (blue). Depositing a layer of 3 u.c. (red) even results in a significantly improved retention of the corresponding devices. However, their resistance still increases by a factor of two within 24 h. Of course, one could expect this trend to continue, when further increasing the SrO thickness. However, considering the already high surface roughness of the stoichiometric film with an additional 3 u.c. of SrO (Fig. 1e)), we decided against a processing of samples with additional 4 u.c.